J Solid State Electrochem (2014) 18:2157–2166
DOI 10.1007/s10008-014-2467-2

ORIGINAL PAPER

Influence of annealing temperature on the electrochemical and surface properties of the 5-V spinel cathode material $LiCr_{0.2}Ni_{0.4}Mn_{1.4}O_4$ synthesized by a sol–gel technique

Reza Younesi · Sara Malmgren · Kristina Edström · Serdar Tan

Received: 7 February 2014 / Revised: 7 March 2014 / Accepted: 19 March 2014 / Published online: 4 April 2014

Abstract $LiCr_{0.2}Ni_{0.4}Mn_{1.4}O_4$ was synthesized by a sol–gel technique in which tartaric acid was used as oxide precursor. The synthesized powder was annealed at five different temperatures from 600 to 1,000 °C and tested as a 5-V cathode material in Li-ion batteries. The study shows that annealing at higher temperatures resulted in improved electrochemical performance, increased particle size, and a differentiated surface composition. Spinel powders synthesized at 900 °C had initial discharge capacities close to 130 mAh g^{-1} at C and C/2 discharge rates. Powders synthesized at 1,000 °C showed capacity retention values higher than 85 % at C/2, C, and 2C rates at 25 °C after 50 cycles. Annealing at 600–800 °C resulted in formation of spinel particles smaller than 200 nm, while almost micron-sized particles were obtained at 900–1,000 °C. Chromium deficiency was detected at the surface of the active materials annealed at low temperatures. The XPS results indicate presence of Cr^{6+} impurity when the annealing temperature was not high enough. The study revealed that increased annealing temperature is beneficial for both improved electrochemical performance of $LiCr_{0.2}Ni_{0.4}Mn_{1.4}O_4$ and for avoiding formation of Cr^{6+} impurity on its surface.

R. Younesi (✉) · S. Malmgren · K. Edström
Department of Chemistry-Ångström Laboratory, Uppsala University, Box 538, SE-75121 Uppsala, Sweden
e-mail: reza.younesi@kemi.uu.se

R. Younesi
Department of Energy Conversion and Storage, Technical University of Denmark, Frederiksborgvej 399, P.O. Box 49, DK-4000 Roskilde, Denmark

S. Tan (✉)
Department of Material Science and Engineering, Akdeniz University, Kampüs Antalya, Dumlupınar Bulvarı, 07058 Antalya, Turkey
e-mail: serdartan@akdeniz.edu.tr

Keywords High voltage · Li–Mn–Ni spinel oxide · Li-ion battery · Cr substitution · Cathode material · Sol–gel

Introduction

Spinel $LiMn_2O_4$ as a 4-V cathode with a capacity of 148 mAh g^{-1} has been considered as a candidate material for the Li-ion battery industry, due to its low cost, abundance, and non-toxicity [1–3]. However, it shows severe capacity fading upon cycling mainly caused by a Jahn–Teller distortion formed during repeated cycling, dissolution of manganese into the electrolyte due to reactions with HF, and oxidation of the organic electrolyte on the electrode [4, 5]. One approach to overcome these problems is partial substitution of manganese by various transition metal ions like Ni^{2+}, Co^{2+}, Fe^{3+}, Cr^{3+}, or Cu^{2+} [1, 4–8]. Among these alternatives, $LiMn_{2-x}Ni_xO_4$ has a dominant high-voltage plateau at 4.7 V while the others exhibit two small plateaus at 4 and 5 V [6, 7, 9–11]. $LiMn_{1.5}Ni_{0.5}O_4$, which shows a comparatively high theoretical discharge capacity (147 mAh g^{-1}) and a relatively stable cyclability, has been intensively investigated as an attractive high-voltage cathode material.

In $LiMn_{1.5}Ni_{0.5}O_4$, O^{2-} anions occupy 32*e* positions in cubic close-packed structure, where the Li^+ ions are located in the 8*a* tetrahedral sites and Ni^{2+} cations replace Mn^{4+} in the 16*d* octahedral sites [12]. The performance of $LiMn_{1.5}Ni_{0.5}O_4$ depends on a number of parameters such as ordering of Mn^{4+} and Ni^{2+} cations, synthesis conditions, and morphology [1, 2]. It has been reported that $LiNi_{0.5}Mn_{1.5}O_4$ synthesized at temperatures higher than 700 °C has low cyclic capacity retention and low 5-V capacity due to formation of oxygen-deficient spinel, Mn^{3+} ions, and impurity phases such as $Li_yNi_{1-y}O$ and NiO [13]. To overcome these problems, different modification techniques such as lattice doping and surface coating have been applied. It has been shown that cationic substitutions could

eliminate formation of the $Li_yNi_{1-y}O$ impurity phase and stabilize the disordered spinel structure, which has superior rate properties compared to the ordered one [14]. So far, several elements like Al [15], Fe [16, 17], Co [16–19], Cr [12, 15, 17, 19–24], Cu [25], Ti [26–28], Ru [29], Mg [16, 30], Zn [16], W [31], and Zr [15] have been examined for this purpose. Among these elements, the addition of Cr has been shown to be more successful than the others to increase cell performance [15, 17]. The electrochemical activity will increase to 4.9 V where the Cr^{3+}/Cr^{4+} redox couple occur [11, 12].

Different techniques have been used to synthesize Cr-substituted $LiNi_{0.5}Mn_{1.5}O_4$. Solid-state reaction of a mixture of carbonates and oxides at 900 °C has been used to synthesize $LiMn_{1.5}Ni_{0.45}Cr_{0.05}O_4$ with a capacity of 130 mAh g^{-1} [32]. Also, mixing acetates and nitrates in an aqueous solution and a subsequent annealing of the precursor at 900 °C have yielded micron-sized $LiMn_{1.4}Ni_{0.4}Cr_{0.2}O_4$ [23]. Also, hydroxide precursor and coprecipitation methods have been used to synthesize $LiMn_{1.4}Ni_{0.4}Cr_{0.2}O_4$ and $LiMn_{1.45}Ni_{0.45}Cr_{0.1}O_4$ [23, 24]. Similarly, a sucrose-aided combustion method has been used which resulted in $LiCr_{0.2}Ni_{0.4}Mn_{1.4}O_4$ powders with capacities higher than 135 mAh g^{-1} [12, 33].

The sol–gel technique offers a versatile route for synthesis of Cr-substituted $LiNi_{0.5}Mn_{1.5}O_4$ [10, 21, 22, 34–37]. According to Yi et al. [22], the gel is a complex network where the metal ions are uniformly distributed in the matrix which prevents phase separation and yields particles with homogeneous size and chemistry. While the technique comprises a number of process parameters, fine-tuning of these parameters allows optimization of the properties of high-voltage cathode materials. Among these parameters, annealing temperature is one of the most important since it will influence the final properties of spinel powder. How the annealing temperature is influencing the properties of Cr-substituted $LiNi_{0.5}Mn_{1.5}O_4$ has been revealed in previous studies by establishing relations between annealing temperature, particle size, and electrochemical properties [20, 27]. However, in these studies, cathode powders were synthesized by techniques other than sol–gel, which resulted in their own process parameter–property relations. In this study, the effect of annealing temperature is systematically investigated to find out its influence on both electrochemical and surface properties of $LiCr_{0.2}Ni_{0.4}Mn_{1.4}O_4$ prepared by sol–gel technique.

Thus, the sol–gel-synthesized powders were annealed from 600 to 1,000 °C for 1 h. Galvanostatic and cyclic voltammetry experiments were performed to analyze the bulk and surface composition of the annealed $LiCr_{0.2}Ni_{0.4}Mn_{1.4}O_4$ powders. Field emission scanning electron microscopy (FE-SEM), X-ray diffraction (XRD), inductively coupled plasma mass spectrometry (ICP-MS), and X-ray photoelectron spectroscopy (XPS) were used to demonstrate how both the bulk structure and the surface composition of the different samples influence the electrochemical stability of the cycling in a Li-ion battery.

Experimental

$LiCr_{0.2}Ni_{0.4}Mn_{1.4}O_4$ was synthesized by a sol–gel method using tartaric acid as an oxide precursor. Stoichiometric amounts of lithium acetate dihydrate [$Li(CH_3COO)\cdot 2H_2O$], manganese acetate tetrahydrate [$Mn(CH_3COO)_2\cdot 4H_2O$], nickel acetate tetrahydrate [$Ni(CH_3COO)_2\cdot 4H_2O$], and chromium nitrate nonahydrate [$Cr(NO_3)_3\cdot 9H_2O$] were dissolved in 20 ml of distilled water to form a solution in which the concentration of nickel acetate was 0.005 mol. All the chemicals were purchased from Sigma-Aldrich. This solution of raw materials was added dropwise to a continuously stirred 1 M tartaric acid solution where the cation/tartaric acid ratio was slightly larger than 1. Finally, pH of the mixture was adjusted to 6.0±0.1 by adding sufficient amount of NH_3 solution. The complete mixture was dried at 55 °C for 24 h and further dried at 120 °C for a few hours until a fine powder was obtained. The collected powder was subsequently ground by mortar and dried in air at 450 °C for 6 h. The resulting precursor powder was ground by mortar again, and five samples of 2.5 g each were annealed in a horizontal tube furnace at either 600, 700, 800, 900, or 1,000 °C for 1 h. Powders were heated to the preselected temperature at a rate of 5 °C min^{-1} and furnace cooled after annealing was complete. X-ray diffraction patterns were obtained using a SIEMENS D5000 Bragg-Brentano X-ray diffractometer employing Cu–K_α radiation (1.54178 Å), with scanning rate of 0.02°/step in 2θ range from 15° to 75°. Surface morphologies of powders were analyzed by LEO (ZEIS) 1550 FE-SEM with 10-kV acceleration voltage and 3–4-mm working distance. XPS samples were prepared by pressing powder into 99.5 % pure aluminum foil using a force corresponding to 1 t. XPS measurements were conducted at an in-house spectrometer (PHI 5500) using monochromatized Al K_α radiation (1486.6 eV) and an electron flood gun to compensate the charging effects. The XPS spectra were energy calibrated by setting the adventitious carbon peak to 285 eV. Bulk composition analyses of synthesized powders were carried out by ICP-MS technique. The samples were digested with microwave digestion system for 20-min ramp to 210 °C, followed by 20-min hold time at 210 °C. To prepare the microwave digestion, 0.05 g of sample, 8 ml HNO_3, 2 ml HF, and 90 ml of deionized water were added into a volumetric flask. Electrochemical characterizations were carried out in vacuum-sealed, polymer-coated aluminum pouch-type cells. Cathodes were fabricated from a slurry of active material, Super P carbon black, and a binder (5 wt.% PVDF in *N*-methyl pyrolidone) in the weight ratio of 75:10:15. The slurry was coated onto an aluminum foil (20-μm thickness, 16.9-mg weight) by doctor-blade deposition. The laminates were dried at 60 °C overnight, and then after, disc-shaped electrodes (20 mm in diameter) were punched out. The electrodes were dried overnight at 120 °C under vacuum inside an Ar-filled glove box (O_2<1 ppm, H_2O

<3 ppm) for 12 h. No pressing was applied on the laminates. A typical electrode thickness and mass were 16–19 μm and 5–6 mg, respectively. Half-cells [Cathode|Solupor® separator soaked in electrolyte|Li foil] were assembled in the same Ar-filled glove box. The electrolyte solution was 1 M $LiPF_6$ in a 1:1 volume ratio mixture of ethylene carbonate (EC) and dimethyl carbonate (DMC). The water content in the electrolyte was determined to be below 10 ppm with Carl Fischer titration. Cyclic voltammetry was performed between 3.00 and 4.99 V (vs. Li/Li^+) at 25 °C at a scan rate of 0.1 mV s^{-1} using a Bio-Logic VMP2 cycling system. Galvanostatic charge–discharge tests with low and high cutoff voltages of 3.00–4.99 V, respectively, were performed at 20 °C using a Digatron BTS-600. Three different current rates of C/2, C, and 2C were used. Multiple measurements were performed at different current rates to calculate the average of discharge capacity. The rates were calculated based on the theoretical capacity of $LiCr_{0.2}Ni_{0.4}Mn_{1.4}O_4$ (147.5 mAh g^{-1}).

Results and discussion

Structural and morphological characterization

XRD patterns of $LiCr_{0.2}Ni_{0.4}Mn_{1.4}O_4$ cathode materials synthesized by a sol–gel technique and annealed at different temperatures are presented in Fig. 1. The diffraction patterns show that all the annealing temperatures yielded pure $LiCr_{0.2}Ni_{0.4}Mn_{1.4}O_4$ without any observable impurity. All peaks in the patterns were identified and labeled according to the cubic space group Fd $\bar{3}$ m. The absence of the (220) diffraction peak at 2θ≈30° indicates that there is no partial occupation of 8*(a)* tetrahedral sites by Mn^{4+}, Ni^{2+}, and Cr^{3+} transition metal cations. Consequently, O^{2-} anions are close-packed in cubic structure where the Li^+ ions are located in the 8*(a)* tetrahedral sites and the Cr^{3+} cations replace Ni^{2+} and Mn^{4+} in the 16*(d)* octahedral sites [18].

Figure 1b shows a comparison of the diffraction patterns of the (400) plane for all the samples. The patterns demonstrate that when the annealing temperature was increased from 600 to 1,000 °C, the width of the peak decreased gradually. In order to show this, full width at half maximum (FWHM) value of the (400) peak was calculated for samples annealed at 800 and 1,000 °C and found as 0.314 and 0.122, respectively. As FWHM value is frequently used as an indicator of the crystal regularity and/or crystallite size [27], it can be stated that those $LiCr_{0.2}Ni_{0.4}Mn_{1.4}O_4$ cathode materials annealed at the higher temperatures have higher crystallinity and/or higher crystallite size (the lattice parameter is about 8.18 Å for the samples annealed above 800 °C). This is in agreement with the results obtained for $LiCr_{0.2}Ni_{0.4}Mn_{1.4}O_4$ powders synthesized by a sucrose-aided combustion technique, which indicates that the crystallinity of powders increases with synthesis temperature [20, 27].

ICP-MS analyses of the synthesized powders (Table 1) showed only the expected elements; no contamination was observed. The ICP-MS results demonstrated that the number of Cr, Ni, and Mn atoms per mole of spinel powders is close to the theoretical values, i.e., 0.2, 0.4, and 1.40, respectively. Some deficiency of the Li could be attributed to the evaporation of Li at the annealing temperature while there is no difference in lithium content as a function of annealing temperature.

FE-SEM images (Fig. 2) of the different $LiCr_{0.2}Ni_{0.4}Mn_{1.4}O_4$ cathode materials show that powders annealed at 600, 700, and 800 °C are primarily composed of particles smaller than 200 nm. The increase in particle size is notable at 900 °C (see Fig. 2d). At this temperature, nano-sized particles disappear while nearly micron-sized polyhedral particles are

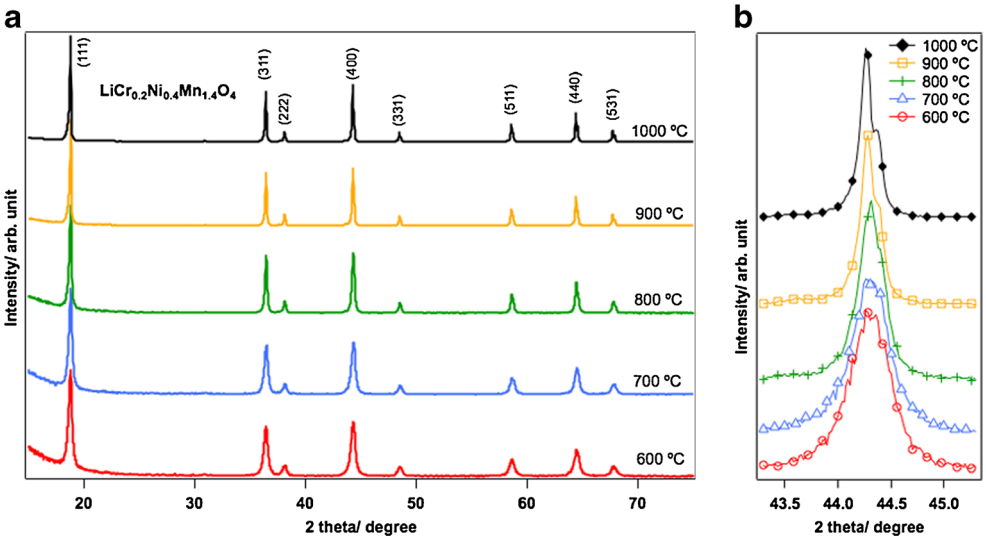

Fig. 1 XRD patterns of $LiCr_{0.2}Ni_{0.4}Mn_{1.4}O_4$ cathode powders synthesized by the sol–gel technique at different temperatures. **a** Diffraction pattern of the powders given for the 2θ range of 10°–75°. **b** Comparison of the (400) diffraction peak for all samples. All patterns were indexed to spinel oxide without any presence of an impurity phase

Table 1 ICP results of the spinel powders. The data show the number of atoms per mole of material

Synthesis temperature (°C)	Li	Cr	Ni	Mn
600	0.94	0.19	0.39	1.39
700	0.94	0.20	0.39	1.38
800	0.94	0.19	0.40	1.38
900	0.95	0.19	0.39	1.39
1,000	0.95	0.20	0.38	1.39

obtained. At 1,000 °C, $LiCr_{0.2}Ni_{0.4}Mn_{1.4}O_4$ particles grow further and reach beyond 1 μm in size. SEM examinations performed in previous studies have yielded similar results. For powders synthesized by the sucrose-aided combustion technique, an increase in the annealing temperature from 700 to 1,100 °C resulted in increase in particle size from 55 nm to 3.2 μm [27]. Also, Sun and co-workers concluded that the growth in particle size was notable above 800 °C when using a hydroxide precursor method [23].

Electrochemical characterization

The electrochemical performance of $LiCr_{0.2}Ni_{0.4}Mn_{1.4}O_4$ spinels was examined at 25 °C by charge/discharge and cyclic voltammetry (CV) studies. Figure 3 displays variations in the discharge capacity and capacity retention values for the first 50 cycles at three different current rates of C/2, C, and 2C for cathodes made out of these powders. Detailed examination of the charge/discharge plots shows that the highest initial discharge capacity, 132 mAh g^{-1}, was attained at C rate for cathodes made from powders annealed at 900 °C. The obtained capacity is about 90 % of theoretical capacity of $LiCr_{0.2}Ni_{0.4}Mn_{1.4}O_4$, which is equal to 147.5 mAh g^{-1}. It should be noted that the same material had 115 mAh g^{-1} discharge capacity at the end of the 50th cycle, which was the highest among all materials examined at all discharge rates in this study.

The capacity retention values (Fig. 3d) of the cathodes imply that at the low discharge rate, C/2, the capacity retention values are higher than 70 % for all active materials. Figure 3a, d demonstrates for C/2 rate that powders synthesized at 900 and 1,000 °C yielded higher initial capacities as well as better capacity retentions than the others. This can be explained by the fact that high-temperature annealing results in bigger particle size and lower surface area, which consequently leads to lower side reactions between the particles and electrolyte. With increasing discharge rate, however, capacity retention values decrease (Fig. 3d) for the powders synthesized at 800, 900, and 1,000 °C. This is commonly observed in rate capability tests of cathode materials [17][20]. However, for the powders synthesized at lower temperatures, 600 and 700 °C, the results from rate capability experiments are not straightforward; the capacity retention increases from C/2 to C and from C to 2C for 600 and 700 °C powders, respectively. This was observed in another work which needs further studies [9]. However, in this study, we expostulate that the presence of Cr^{6+} in powders synthesized at lower temperature (shown later in the XPS results) might cause these unpredictable rate capability results due to side reactions.

It should be emphasized that among all the five $LiCr_{0.2}Ni_{0.4}Mn_{1.4}O_4$ materials, the one synthesized at 1,000 °C is superior to all the others in terms of capacity

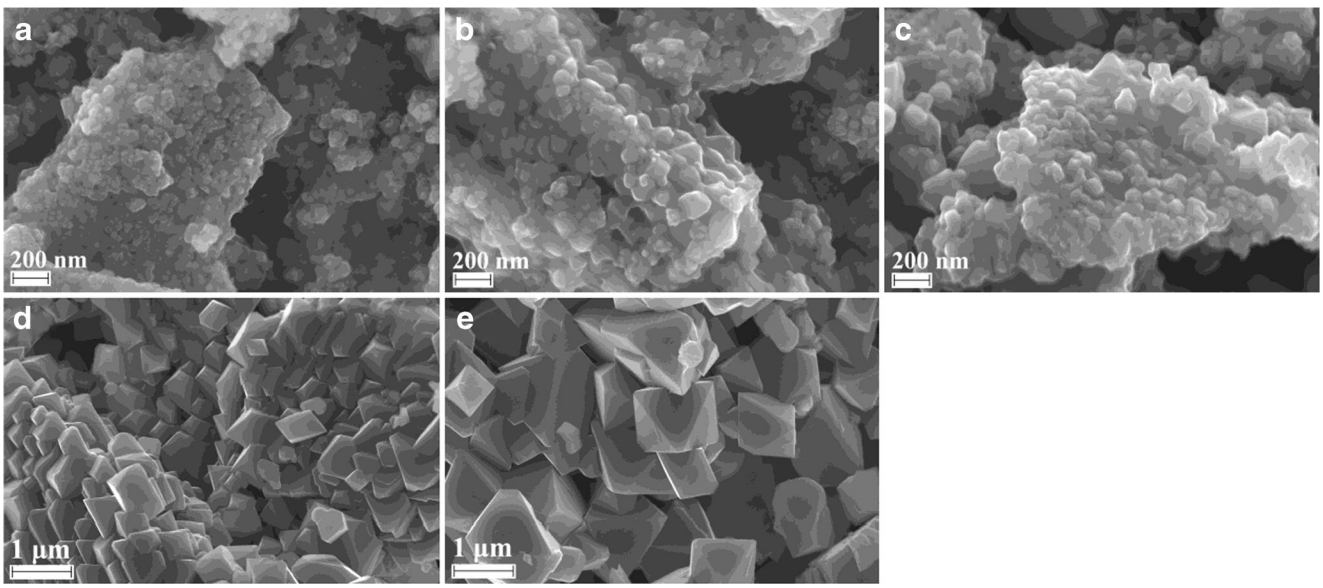

Fig. 2 FE-SEM images of $LiCr_{0.2}Ni_{0.4}Mn_{1.4}O_4$ powders synthesized by the sol–gel technique and annealed at different temperatures of **a** 600, **b** 700, **c** 800, **d** 900, and **e** 1,000 °C

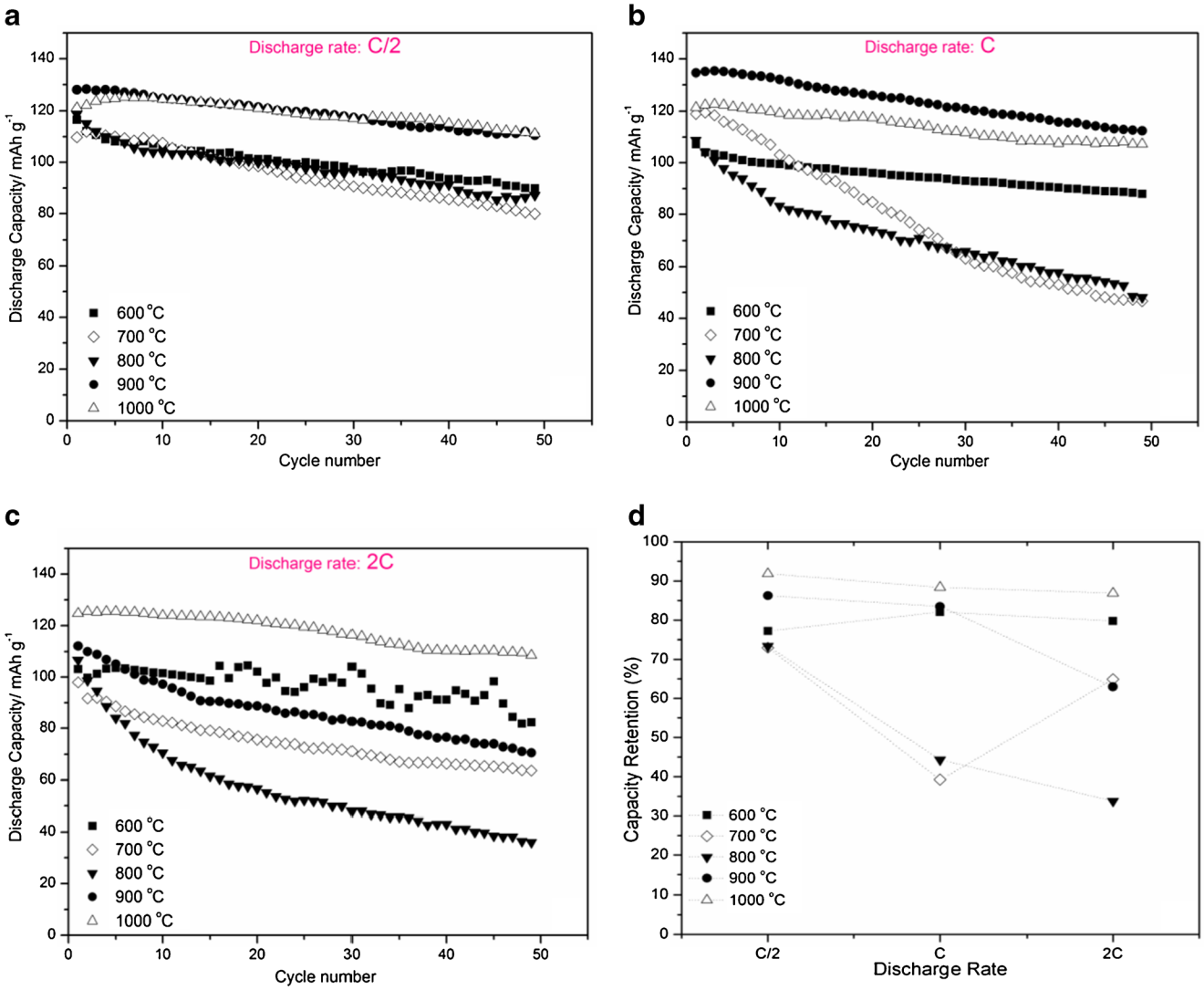

Fig. 3 Discharge capacity for $LiCr_{0.2}Ni_{0.4}Mn_{1.4}O_4$ powders synthesized by the sol–gel technique, annealed at different temperatures, and cycled at C/2 (**a**), C (**b**), and 2C (**c**) rates, as well as the capacity retention after 50 cycles (**d**) for cells cycled at the different rates

retention at all discharge rates, showing a discharge capacity higher than 120 mAh g^{-1} with a capacity retention higher than 85 % after 50 cycles (Fig. 3d). It has been shown that annealing at high temperatures can improve performance of Cr-substituted LNMO materials. Indeed, in most of the papers mentioned in Table 2, a high-temperature annealing at about 800–900 °C was used. Similarly, it has been published for different synthesis techniques (e.g., sucrose-aided combustion and hydroxide precursor methods) that heat treatment at temperatures higher than 800 °C improves the electrochemical performance of Cr-substituted $LiNi_{0.5}Mn_{1.5}O_4$ powder [12, 20]. In these previous studies, however, the authors have mainly attributed the increase in discharge capacity and capacity retention to particle growth combined with an increased crystallinity of the spinel powders [38].

A summary of published results regarding the cyclic performance of Cr-substituted $LiNi_{0.5}Mn_{1.5}O_4$ synthesized by sol–gel technique is presented in Table 2. At the current rate of 0.5 C, discharge capacities between 130 and 140 mAh g^{-1} were reported [10, 34], which are comparable to our results. A discharge capacity of ~140 mAh g^{-1} has been reported for Cr-substituted $LiNi_{0.5}Mn_{1.5}O_4$ cathode material [19, 21]. However, those values were acquired at lower discharge rates (e.g., 0.2 C) or number of cycles (e.g., 20 cycles) compared to results obtained in this study at a relatively higher current rate. The initial discharge capacity is higher in this study compared to the other published results [34, 36].

As powders annealed at 800, 900, and 1,000 °C yielded more promising charge/discharge behavior than the others, they were examined by cyclic voltammetry in more detail. Figure 4 illustrates cyclic voltammograms for $LiCr_{0.2}Ni_{0.4}Mn_{1.4}O_4$ powders annealed at 800, 900, and 1,000 °C. In order to see the effect of cycling, the first and tenth cycles are presented in the

Table 2 A short summary comparing our results with reported cyclic performance of Cr-substituted $LiNi_{0.5}Mn_{1.5}O_4$ synthesized by a sol–gel technique

Number	Material	Annealing temperature	Current rate (C)	Voltage range (V)	Discharge capacity (mAh g^{-1})		Reference
					First cycle	50th cycle	
1	$LiCr_{0.05}Ni_{0.45}Mn_{1.5}O_4$	12 h at 600 °C+24 h at 800 °C	0.5	3.5–5	137	134	[10]
2	$LiCr_{0.1}Ni_{0.45}Mn_{1.45}O_4$	4 h at 400 °C+10 h at 700 °C	0.2	3.5–5	140	–	[19]
3	$LiCr_{0.1}Ni_{0.4}Mn_{1.5}O_4$	5 h at 450 °C+15 h at 900 °C	~0.3	3.5–5.2	144	–	[21]
4	$LiCr_{0.2}Ni_{0.4}Mn_{1.4}O_4$	12 h at 110 °C+20 h at 850 °C	0.15	3.5–4.98	130	127	[22]
5	$LiCr_{0.1}Ni_{0.4}Mn_{1.5}O_4$	8 h at 900 °C	0.5 1	3.5–5	141 125	139 122	[34]
6	$LiCr_{0.25}Ni_{0.25}Mn_{1.5}O_4$	8 h at 850 °C	0.1	3–5	110	–	[35]
7	$LiCr_{0.1}Ni_{0.4}Mn_{1.5}O_4$	4 h at 450 °C+24 h at 875 °C	0.2 0.5 1	3–4.9	108 95 62	124 103 92	[36]
8	$LiCr_{0.2}Ni_{0.4}Mn_{1.4}O_4$	24 h at 850 °C	0.15	3.3–4.95	131	128	[37]
9	$LiCr_{0.2}Ni_{0.4}Mn_{1.4}O_4$	1 h at 900 °C	0.5 1	3–4.99	129 135	112 118	This work

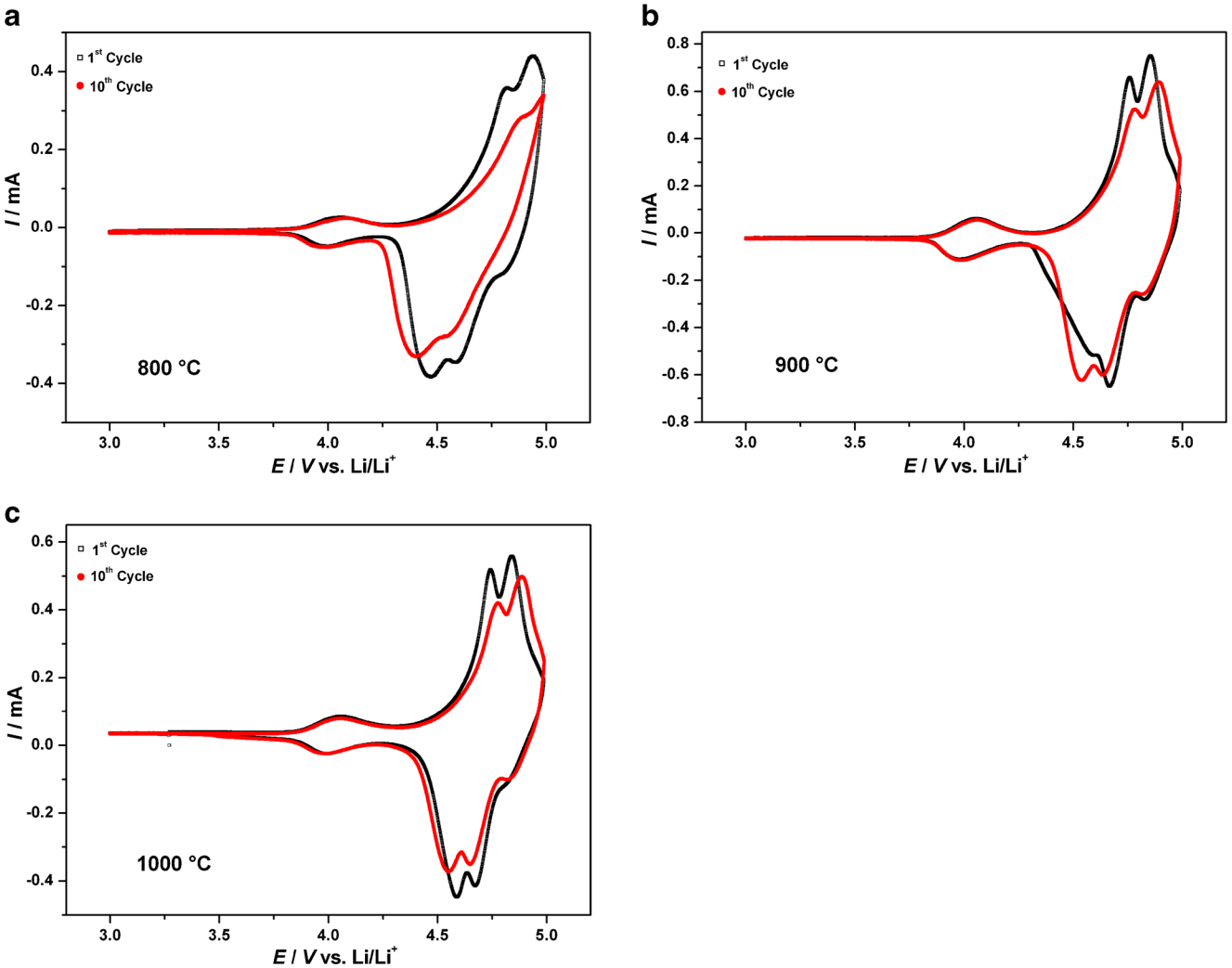

Fig. 4 Cyclic voltammograms for $LiCr_{0.2}Ni_{0.4}Mn_{1.4}O_4$ powders annealed at 800 (**a**), 900 (**b**), and 1,000 °C (c), respectively. Each plot shows the first and tenth cycle to illustrate the variation in electrochemical activity with cycling. Oxidation reactions are observed at around 4 V (Mn^{3+}/Mn^{4+}), 4.75 V (Ni^{2+}/Ni^{3+}), 4.85 V (Ni^{3+}/Ni^{4+}), and 5.0 V (Cr^{3+}/Cr^{4+}) vs. Li/Li^+, respectively. Scan rate is 0.1 mV s^{-1}

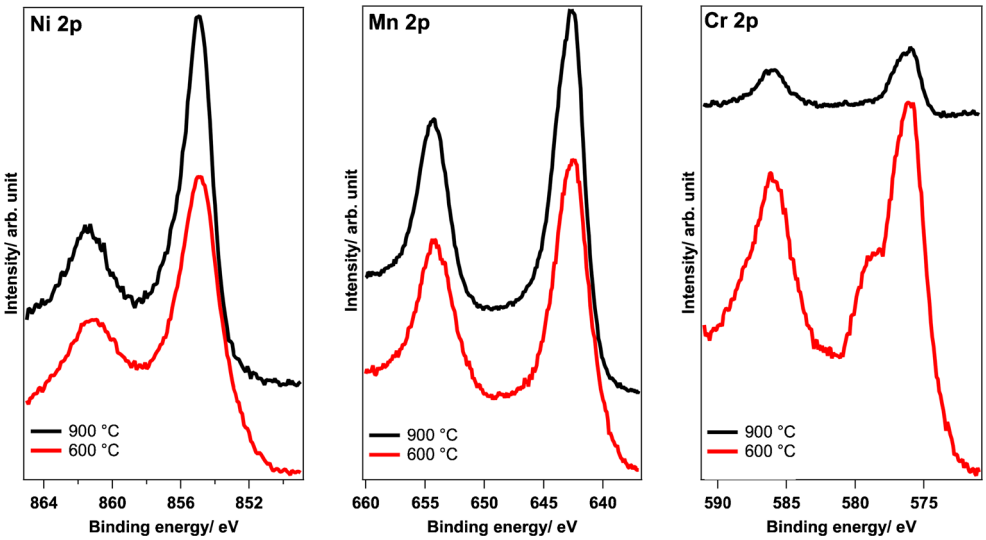

Fig. 5 Ni2p, Mn2p, and Cr2p spectra of $LiCr_{0.2}Ni_{0.4}Mn_{1.4}O_4$ powders annealed at 600 and 900 °C

same plots. A reversible electrochemical activity could be observed around 4 V. This can be attributed to the Mn^{3+}/Mn^{4+} redox couple showing that the as-synthesized $LiCr_{0.2}Ni_{0.4}Mn_{1.4}O_4$ powders contain some Mn^{3+} [28]. Furthermore, two reversible peaks at 4.75 and 4.87 V with minor variations appear in the graphs. These peaks are related with Ni^{2+}/Ni^{3+} and Ni^{3+}/Ni^{4+} activities, respectively [21]. Additionally, there is a shoulder close to 5 V in CVs of the samples annealed at 900 and 1,000 °C, which is possibly an indication of Cr^{3+}/Cr^{4+} activity [17]. In fact, in the reduction sweep of all materials, there is a signal at ca. 4.9 V representing an activity other than reduction of Mn and Ni. This signal was previously reported as Cr^{4+}/Cr^{3+} reduction [17] indicating that Cr is an electrochemically active element in the synthesized spinel samples.

Another important electrochemical property of the $LiCr_{0.2}Ni_{0.4}Mn_{1.4}O_4$ cathode material is the available power offered by this material during discharge. This can be obtained by integrating the area under the *I–V* curves of reduction sweeps in voltammograms. Figure 4 shows that the high voltage contribution, i.e., electrochemical activities of Ni and Cr, dominates the available power. For all samples examined by cyclic voltammetry, low-voltage (Mn^{4+}/Mn^{3+}) activity comprises less than 15 % which means that the spinel materials mainly offer high-voltage power.

There are also some differences between the first and tenth cycles of the voltammograms shown in Fig. 4. The oxidation peaks of Ni slightly shift to higher voltages upon cycling, while the voltage of the Mn^{3+} oxidation remains constant. Similarly, Ni peaks shift to lower voltage values on reduction, while the positions of the Mn^{4+} and Cr^{4+} peaks remain constant. Furthermore, the peak current and total area under the curves slightly decrease from the first to the tenth cycle showing a small decrease in electrochemical activity of the spinel electrodes. The loss in electrochemical activity is more pronounced for the sample annealed at 800 °C compared to the samples annealed at higher temperatures. It should be noted that this decrease in the peak current values and the total area under the curves was observed only at voltages higher than 4.25 V, while Mn^{3+}/Mn^{4+} redox activity around 4.0 V was stable even after ten cycles regardless of the annealing temperature.

The overall evaluation of the CV results of this study requires the comparison of the collected data with theoretical and previously reported ones. According to Aklalouch and

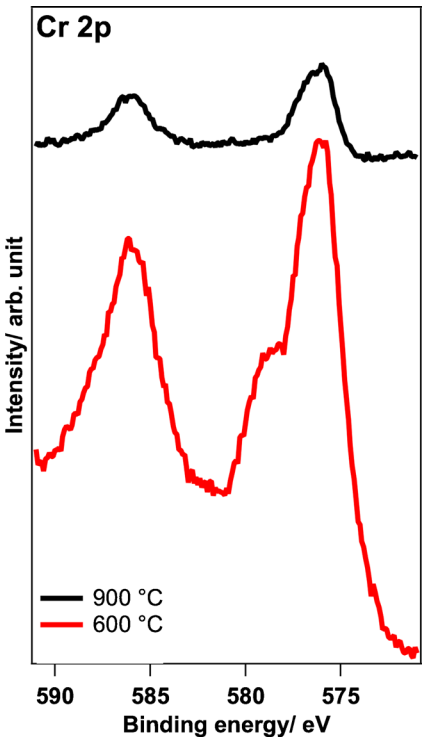

Fig. 6 Cr2p spectra normalized with respect to the 576-eV feature for $LiCr_{0.2}Ni_{0.4}Mn_{1.4}O_4$ powders annealed at 600 and 900 °C

coworkers [27], the oxidation sweep in the CV meaning the removal of Li during charging of $LiCr_{0.2}Ni_{0.4}Mn_{1.4}O_4$ can ideally be described by the following reaction:

$$LiCr^{3+}_{0.2}Ni^{2+}_{0.4}Mn^{4+}_{1.4}O_4 \xrightarrow{\text{charging}} Cr^{4+}_{0.2}Ni^{4+}_{0.4}Mn^{4+}_{1.4}O_4 + Li^+ + e^-$$

This removal of a Li^+ ion from the spinel phase results in oxidation of Ni^{2+} to Ni^{3+}, Ni^{3+} to Ni^{4+}, and Cr^{3+} to Cr^{4+}, while Mn^{4+} is electrochemically inactive. However, the results obtained in this study demonstrate that as-synthesized powders also have Mn^{3+}/Mn^{4+} activity showing that the real oxidation sweep of these powders is different from the above reaction formula. In fact, Mn^{3+}/Mn^{4+} redox activity of Cr-substituted $LiNi_{0.5}Mn_{1.5}O_4$ has also been observed in other studies. According to Katiyar et al. [35], both (a) the overall electrochemical activity detected for the $LiCr_{0.1}Ni_{0.4}Mn_{1.5}O_4$ cathodes and (b) the contribution of $Mn^{3+/}Mn^{4+}$ redox couple to this activity increase during the first ten cycles. This was attributed to electrochemical activation of the cathode powder and higher lithium utilization upon cycling. In the present study, the Mn activity did not change with cycling while its contribution to the overall electrochemical activity increased due to the decrease in Ni^{2+}/Ni^{4+} activities.

One important feature of the cyclic CV results given in Fig. 4 is the reduction of the peak current upon cycling. This can be clearly seen for the sample annealed at 800 °C (see Fig. 4a). According to Liu et al. [32], the diffusion coefficient of Li^+ in the spinel cathode material is directly proportional to the second power of the peak current density of the voltammetry. Thus, it can be stated that a slight decrease in the Li^+ diffusion occurs upon cycling of the $LiCr_{0.2}Ni_{0.4}Mn_{1.4}O_4$ powders. This decrease is more noticeable for the sample annealed at 800 °C compared to the other samples annealed at the higher temperatures. This more pronounced reduction in the diffusion coefficient of Li^+ could be attributed to the lower stability of the spinel structure at lower annealing temperatures. It should be noted that other than attaining high capacity and capacity retention values, this is another reason why high-temperature annealing is beneficial in the synthesis of $LiCr_{0.2}Ni_{0.4}Mn_{1.4}O_4$ cathode material by sol–gel technique.

Surface characterization

As it is presented above, the bulk composition of all the synthesized powders were close to the theoretical composition of $LiCr_{0.2}Ni_{0.4}Mn_{1.4}O_4$ (see Table 1 for the results of ICP-MS analyses). In order to estimate the surface composition of these powders, XPS was used. For clarity, only spectra for the two extremes, the samples annealed at 600 and 900 °C, are given in Fig. 5. The Ni2p and Mn2p spectra are similar for both powders representing Ni^{2+} and Mn^{4+} [35, 39], while the Cr2p spectra are clearly different. The relative intensity of the Cr2p spectrum is higher for the powder annealed at 600 °C compared to that at 900 °C, indicating a lower chromium content in the surface of the sample annealed at higher temperature. Also, the shape of the Cr2p spectra differs for samples synthesized at different temperatures.

To better illustrate these differences, Fig. 6 presents Cr2p spectra normalized with respect to the highest intensity feature at 576 eV attributed to Cr^{3+} [40]. There is a peak at 579 eV attributed to Cr^{6+} on the surface of the powder annealed at 600 °C. It has previously been shown for $LiMn_{2-y}Cr_yO_4$ that Cr^{3+} converts to Cr^{6+} when $y>0.2$ [41]. Also, formation of Cr^{6+} has been observed during cycling of $Li_{1.2}Cr_{0.4}Mn_{0.4}O_2$ [42] and $LiMn_{0.4}Cr_{0.2}Ni_{0.4}O_2$ [43]. However, to our knowledge, no influence on the relative Cr^{6+} content of the annealing temperature has previously been shown for $LiCr_xNi_yMn_{2-x-y}O_4$ powders. Thus, the increased annealing temperature can be concluded to be beneficial to avoid formation of Cr^{6+} impurity.

Conclusion

This study reveals for $LiCr_{0.2}Ni_{0.4}Mn_{1.4}O_4$ powder synthesized by sol–gel technique that annealing at temperatures higher than 800 °C is beneficial for improving the discharge capacity and capacity retention of this 5-V cathode material. Li-ion batteries assembled with $LiCr_{0.2}Ni_{0.4}Mn_{1.4}O_4$ powder annealed at 900 °C exhibited a discharge capacity close to 130 mAh g^{-1} at C and C/2 current rates. Examination of structural, morphological, and electrochemical properties points out that high-temperature annealing led to increase in particle size and to stability of spinel structure of powder. XPS results showed presence of Cr^{6+} impurity on the surface of the spinel powder when the annealing temperature was low (600 °C). However, no Cr^{6+} was observed on the surface of powder annealed at high temperature (900 °C). Thus, an annealing stage at temperatures higher than 800 °C can be used to improve performance of $LiCr_{0.2}Ni_{0.4}Mn_{1.4}O_4$ cathode material synthesized by sol–gel.

Acknowledgments Serdar Tan was supported by The Scientific and Technological Research Council of Turkey (TUBITAK) during this study, which authors acknowledge. The work was also supported by the Swedish Research Council, Contract 2009-3345, and the Swedish Strategic Research Program STandUp for Energy.

References

1. Santhanam R, Rambabu B (2010) Research progress in high voltage spinel $LiNi_{0.5}Mn_{1.5}O_4$ material. J Power Sources 195:5442–5451
2. Liu GQ, Wen L, Liu YM (2010) Spinel $LiNi_{0.5}Mn_{1.5}O_4$ and its derivatives as cathodes for high-voltage Li-ion batteries. J Solid State Electrochem 14:2191–2202
3. Hosono E, Kudo T, Honma I, Matsuda H, Zhou H (2009) Synthesis of single crystalline spinel $LiMn_2O_4$ nanowires for a lithium ion battery with high power density. Nano Lett 9:1045–1051
4. Gummow RJ, de Kock A, Thackeray MM (1994) Improved capacity retention in rechargeable 4 V lithium/lithium–manganese oxide (spinel) cells. Solid State Ionics 69:59–67
5. Amine K, Tukamoto H, Yasuda H, Fujita Y (1996) A new three-volt spinel $Li_{1+x}Mn_{1.5}Ni_{0.5}O_4$ for secondary lithium batteries. J Electrochem Soc 143:1607–1613
6. Kawai H, Nagata M, Kageyama H, Tukamoto H, West AR (1999) 5 V lithium cathodes based on spinel solid solutions Li2Co1+ XMn3–XO8:−1≤X≤1. Electrochim Acta 45:315–327
7. Zhong Q, Bonakdarpour A, Zhang M, Gao Y, Dahn JR (1997) Synthesis and electrochemistry of $LiNi_xMn_{2-x}O_4$. J Electrochem Soc 144:205–213
8. Morales J, Sánchez L, Tirado JL (1998) New doped Li–M–Mn–O (M=Al, Fe, Ni) spinels as cathodes for rechargeable 3 V lithium batteries. J Solid State Electrochem 2:420–426
9. Kim Y, Dudney NJ, Chi M, Martha SK, Nanda J, Veith GM, Liang C (2013) A perspective on coatings to stabilize high-voltage cathodes: $LiMn_{1.5}Ni_{0.5}O_4$ with sub-nanometer lipon cycled with $LiPF_6$ electrolyte. J Electrochem Soc 160:A3113–A3125
10. Bin PS, Eom WS, Cho WI, Jang H (2006) Electrochemical properties of $LiNi_{0.5}Mn_{1.5}O_4$ cathode after Cr doping. J Power Sources 159: 679–684
11. Sigala C, Verbaere A, Mansot JL, Guyomard D, Piffar Y, Tournoux M (1997) The Cr-substituted spinel Mn oxides $LiCr_yMn_{2-y}O_4$($0\le y\le 1$): Rietveld analysis of the structure modifications induced by the electrochemical lithium deintercalation. J Solid State Chem 132:372–381
12. Aklalouch M, Amarilla JM, Rojas RM, Saadoune I, Rojo JM (2008) Chromium doping as a new approach to improve the cycling performance at high temperature of 5 V $LiNi_{0.5}Mn_{1.5}O_4$-based positive electrode. J Power Sources 185:501–511
13. Xiao J, Chen X, Sushko PV, Sushko ML, Kovarik L, Feng J, Deng Z, Zheng J, Graff GL, Nie Z, Choi D, Liu J, Zhang J-G, Whittingham MS (2012) High-performance $LiNi_{0.5}Mn_{1.5}O_4$ spinel controlled by Mn^{3+} concentration and site disorder. Adv Mater 24:2109–2116
14. Yi T-F, Xie Y, Ye M-F, Jiang L-J, Zhu R-S, Zhu Y-R (2011) Recent developments in the doping of $LiNi_{0.5}Mn_{1.5}O_4$ cathode material for 5 V lithium-ion batteries. Ionics (Kiel) 17:383–389
15. Oh SH, Chung KY, Jeon SH, Kim CM, Cho WI, Cho BW (2009) Structural and electrochemical investigations on the $LiNi_{0.5-x}Mn_{1.5-y}M_{x+y}O4$ (M=Cr, Al, Zr) compound for 5 V cathode material. J Alloys Compd 469:244–250
16. Arunkumar TA, Manthiram A (2005) Influence of lattice parameter differences on the electrochemical performance of the 5 V spinel $LiMn_{1.5-y}Ni_{0.5-z}M_{y+z}O_4$ (M=Li, Mg, Fe, Co, and Zn). Electrochem Solid-State Lett 8:A403–A405
17. Zhong GB, Wang YY, Yu YQ, Chen CH (2012) Electrochemical investigations of the $LiNi_{0.45}M_{0.10}Mn_{1.45}O_4$ (M=Fe, Co, Cr) 5 V cathode materials for lithium ion batteries. J Power Sources 205:385–393
18. Jang M-W, Jung H-G, Scrosati B, Sun Y-K (2012) Improved co-substituted, $LiNi_{0.5-x}Co_{2x}Mn_{1.5-x}O_4$ lithium ion battery cathode materials. J Power Sources 220:354–359
19. Kawai N, Nakamura T, Yamada Y, Tabuchi M (2011) Electrochemical and magnetic studies of Cr3+- or Co3+-substituted Li–Mn–Ni spinel oxides. J Power Sources 196:6969–6973
20. Liu D, Lu Y, Goodenough JB (2010) Rate properties and elevated-temperature performances of $LiNi_{0.5-x}Cr_{2x}Mn_{1.5-x}O_4$ ($0\le 2x\le 0.8$) as 5 V cathode materials for lithium-ion batteries. J Electrochem Soc 157:A1269–A1273
21. Hong K-J, Sun Y-K (2002) Synthesis and electrochemical characteristics of $LiCr_xNi_{0.5-x}Mn_{1.5}O_4$ spinel as 5 V cathode materials for lithium secondary batteries. J Power Sources 109:427–430
22. Yi T-F, Li C-Y, Zhu Y-R, Shu J, Zhu R-S (2009) Comparison of structure and electrochemical properties for 5 V $LiNi_{0.5}Mn_{1.5}O_4$ and $LiNi_{0.4}Cr_{0.2}Mn_{1.4}O_4$ cathode materials. J Solid State Electrochem 13: 913–919
23. Arunkumar TA, Manthiram A (2005) Influence of chromium doping on the electrochemical performance of the 5 V spinel cathode $LiMn_{1.5}Ni_{0.5}O_4$. Electrochim Acta 50:5568–5572
24. Sun Y, Wang Z, Huang X, Chen L (2004) Synthesis and electrochemical performance of spinel $LiMn_{2-x-y}Ni_xCr_yO_4$ as 5-V cathode materials for lithium ion batteries. J Power Sources 132:161–165
25. Yang M-C, Xu B, Cheng J-H, Pan C-J, Hwang B-J, Meng YS (2011) Electronic, structural, and electrochemical properties of $LiNi_xCu_yMn_{2-x-y}O_4$ ($0<x<0.5$, $0<y<0.5$) high-voltage spinel materials. Chem Mater 23:2832–2841
26. Alcántara R, Jaraba M, Lavela P, Tirado JL (2003) Structural and electrochemical study of new $LiNi_{0.5}Ti_xMn_{1.5-x}O_4$ spinel oxides for 5-V cathode materials. Chem Mater 15:2376–2382
27. Lin M, Wang SH, Gong ZL, Huang XK, Yang Y (2013) A strategy to improve cyclic performance of $LiNi_{0.5}Mn_{1.5}O_4$ in a wide voltage region by Ti-doping. J Electrochem Soc 160:A3036–A3040
28. Le M-L-P, Strobel P, Alloin F, Pagnier T (2010) Influence of the tetravalent cation on the high-voltage electrochemical activity of $LiNi_{0.5}M_{1.5}O_4$ spinel cathode materials. Electrochim Acta 56:592–599
29. Wang H, Tan TA, Yang P, Lai MO, Lu L (2011) High-rate performances of the Ru-doped spinel $LiNi_{0.5}Mn_{1.5}O_4$: effects of doping and particle size. J Phys Chem C 115:6102–6110
30. Shiu J-J, Pang WK, Wu S (2013) Preparation and characterization of spinel $LiNi_{0.5-x}Mg_xMn_{1.5}O_4$ cathode materials via spray pyrolysis method. J Power Sources 244:35–42
31. Prabakar SJR, Han SC, Singh SP, Lee DK, Sohn K-S, Pyo M (2012) W-doped $LiW_xNi_{0.5}Mn_{1.5-x}O_4$ cathodes for the improvement of high rate performances in Li ion batteries. J Power Sources 209:57–64
32. Xu W, Chen X, Ding F, Xiao J, Wang D, Pan A, Zheng J, Li XS, Padmaperuma AB, Zhang J-G (2012) Reinvestigation on the state-of-the-art nonaqueous carbonate electrolytes for 5 V Li-ion battery applications. J Power Sources 213:304–316
33. Ju SH, Kim D-W (2013) Effect of calcination temperature on the structure and electrochemical performance of $LiMn_{1.5}Ni_{0.5}O_4$ cathode materials. Bull Korean Chem Soc 34:59–62
34. Liu GQ, Wen L, Liu GY, Tian YW (2010) Rate capability of spinel $LiCr_{0.1}Ni_{0.4}Mn_{1.5}O_4$. J Alloys Compd 501:233–235
35. Rajakumar S, Thirunakaran R, Sivashanmugam A, Yamaki J-I, Gopukumar S (2009) Electrochemical behavior of $LiM_{0.25}Ni_{0.25}Mn_{1.5}O_4$ as 5 V cathode materials for lithium rechargeable batteries. J Electrochem Soc 156:A246–A252
36. Katiyar RK, Singhal R, Asmar K, Valentin R, Katiyar RS (2009) High voltage spinel cathode materials for high energy density and high rate capability Li ion rechargeable batteries. J Power Sources 194:526–530
37. Yi T-F, Shu J, Zhu Y-R, Zhu R-S (2009) Advanced electrochemical performance of $LiMn_{1.4}Cr_{0.2}Ni_{0.4}O_4$ as 5 V cathode material by citric-acid-assisted method. J Phys Chem Solids 70:153–158
38. Aklalouch M, Rojas RM, Rojo JM, Saadoune I, Amarilla JM (2009) The role of particle size on the electrochemical properties at 25 and at 55 °C of the $LiCr_{0.2}Ni_{0.4}Mn_{1.4}O_4$ spinel as 5 V-cathode materials for lithium-ion batteries. Electrochim Acta 54:7542–7550
39. Younesi R, Urbonaite S, Edström K, Hahlin M (2012) The cathode surface composition of a cycled Li–O_2 battery: a photoelectron spectroscopy study. J Phys Chem C 116:20673–20680

40. Oswald S, Nikolowski K, Ehrenberg H (2010) XPS investigations of valence changes during cycling of $LiCrMnO_4$-based cathodes in Li-ion batteries. Surf Interface Anal 42:916–921
41. Wu C, Wu F, Chen L, Huang X (2002) X-ray diffraction and X-ray photoelectron spectroscopy analysis of Cr-doped spinel $LiMn_2O_4$ for lithium ion batteries. Solid State Ionics 152–153:335–339
42. Balasubramanian M, McBreen J, Davidson IJ, Whitfiel PS, Kargina I (2002) In situ x-ray absorption study of a layered manganese–chromium oxide-based cathode material. J Electrochem Soc 149:A176
43. Karan NK, Balasubramanian M, Abraham DP, Furczon MM, Pradhan DK, Saavedra-Arias JJ, Thomas R, Katiyar RS (2009) Structural characteristics and electrochemical performance of layered $Li[Mn_{0.5-x}Cr_{2x}Ni_{0.5-x}]O2$ cathode materials. J Power Sources 187:586–590